Deoxyadenosine–Deoxycytidine Pairing in the d(C-G-C-G-A-A-T-T-C-A-C-G) Duplex: Conformation and Dynamics at and Adjacent to the dA·dC Mismatch Site†

Dinshaw J. Patel,* Sharon A. Kozlowski, Satoshi Ikuta, and Keiichi Itakura

ABSTRACT: Deoxyadenosine–deoxycytidine pairing at symmetrically related dA·dC mismatch sites in the d(C_1-G_2-C_3-G_4-A_5-A_6-T_6-T_5-C_4-A_3-C_2-G_1) self-complementary duplex (henceforth called 12-mer AC) has been investigated by proton and phosphorus NMR studies in aqueous solution. We demonstrate that base pairing is maintained on either side of the mismatch site in the 12-mer AC duplex at low temperature. The proton chemical shifts and NOE measurements rule out models in which the H-2 proton of adenosine at the mismatch site is stacked over adjacent dG·dC base pairs. A comparison of the hydrogen-exchange kinetics in the d(C-G-C-G-A-A-T-T-C-G-C-G) duplex (henceforth called 12-mer) with standard dG·dC base pairs at position 3 from either end with the 12-mer AC duplex, which contains dA·dC mismatches at these positions, demonstrates kinetic destabilization at dG·dC base pair 4 adjacent to the mismatch site and at dA·dT base pairs 5 and 6 far from this site. This contrasts with previous hydrogen-exchange studies on the 12-mer GT and 12-mer GA duplexes where the kinetic destabilization was localized to base pair 4, which is adjacent to the mispairing site. The melting temperature of the 12-mer AC duplex in 0.1 M phosphate is ~30 °C lower than the corresponding value for the 12-mer duplex. This indicates that the overall duplex stability is affected to a greater degree on replacing two dG·dC base pairs by dA·dC pairs compared to replacement by either dG·dT or dG·dA pairs. Perturbations in the phosphodiester backbone of the 12-mer AC duplex can be readily detected by the observation of a downfield-shifted resolved phosphorus resonance assigned tentatively to a phosphate at the mismatch site.

Purine–pyrimidine pairing is a central feature of the DNA double helix. In addition to the standard Watson–Crick dG·dC and dA·dT pairs, one can generate the wobble dG·dT pair in the interior of DNA duplexes (Early et al., 1978; Patel et al., 1982a). The proposed dG·dT hydrogen-bonding scheme involves two imino to carbonyl hydrogen bonds with the guanosine H-1 and thymidine H-3 imino protons participating in the pairing interaction (Redfield et al., 1981; Reid, 1981; Patel et al., 1982a).

The situation gets more complicated for purine–pyrimidine pairs involving dA and dC residues (Wallace et al., 1979), neither of which contains an imino proton in the keto tautomeric form. Various models have considered keto and enol isomers and the anti and syn configurations about the glycosidic bond (Lomant & Fresco, 1975; Rein et al., 1983), but these proposals must be treated with caution in the absence of experimental information that defines the orientation of bases and the groups involved in the hydrogen bonding.

We have set out to systematically investigate the introduction of base-pair mismatches at position 3 from either end of the d(C_1-G_2-C_3-G_4-A_5-A_6-T_6-T_5-C_4-G_3-C_2-G_1) self-complementary duplex (henceforth called 12-mer) (Patel et al., 1982b). Our initial efforts were directed toward elucidation of the dG·dT wobble pairing scheme (Patel et al., 1982a), and more recently, we have investigated the dG·dA pair in which both purine bases adopt the anti configuration [Kan et al., 1983; see preceding paper (Patel et al., 1984)]. This paper reports on a proton and phosphorus NMR investigation of the d(C-G-C-G-A-A-T-T-C-A-C-G) self-complementary duplex (Chart I; henceforth designated 12-mer AC duplex) in which two dA·dC interactions replace two dG·dC pairs at position 3 from either end of the duplex.

Chart I

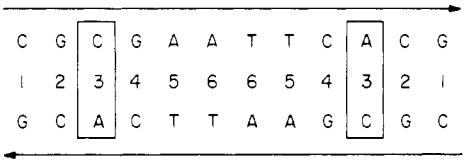

Experimental Procedures

NMR Spectroscopy. Proton spectra were recorded on an XL-200 MHz and the 498-MHz NMR spectrometer at the Francis Bitter National Magnet Laboratory, MIT. Phosphorus spectra were recorded on an XL-200 spectrometer.

Synthesis. The 12-mer AC sequence was synthesized in milligram amounts by the solid-phase triester method reported previously (Tan et al., 1983). Dinucleotides were added through their 3′ ends to the growing nucleotide chain on the polystyrene copolymer support. The dimer couplings to yield the 12-mer AC sequence were undertaken with percentage yields of 88, 90, 93, 89, and 90, respectively, on proceeding from the 3′ to the 5′ end. The final product was cleaved from the solid support, the protecting group deblocked, and the 12-mer AC purified on DEAE-cellulose DE-52 followed by size-exclusion chromatography on G-75 or G-50. This procedure yielded 129 A_{260} units of the 12-mer AC sequence. The high-temperature proton NMR spectrum of the 12-mer AC confirmed the purity of the dodecanucleotide.

Concentration. The proton NMR spectra were recorded on 129 A_{260} units of 12-mer AC in 0.2 mL of 0.1 M phosphate buffer. The samples were diluted by a factor of 2 to record

† From AT&T Bell Laboratories, Inc., Murray Hill, New Jersey 07974 (D.J.P. and S.A.K.), and the Molecular Genetics Department, City of Hope National Medical Center, Duarte, California 91010 (S.I. and K.I.). *Received November 7, 1983.* The high-field NMR experiments were performed at the NMR facility for biomedical research located at the Francis Bitter National Magnet Laboratory, Massachusetts Institute of Technology. The NMR facility is supported by Grant RR0095 from the Division of Research Resources (National Institutes of Health) and by the National Science Foundation under Contract C-670. The contributions of S.I. and K.I. were funded by NIH Grant 28651.

0006-2960/84/0423-3218$01.50/0

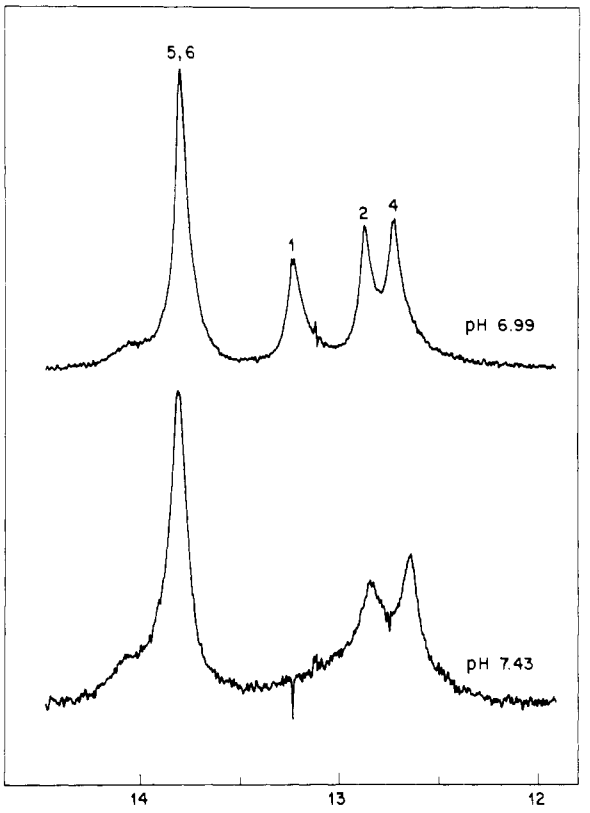

FIGURE 1: The 498-MHz proton NMR spectra of the 12-mer AC duplex in 0.1 M phosphate, 2.5 mM ethylenediaminetetraacetic acid (EDTA), and 4:1 H_2O–D_2O at pH 6.99 and −6 °C (top) and pH 7.43 and −5 °C (bottom).

Table I: A Comparison of the Imino Proton Chemical Shifts in the 12-mer and 12-mer AC Duplexes at −5 °C

	chemical shift (ppm)	
base pair	12-mer[a]	12-mer AC[b]
dG·dC 1	13.29	13.23
dG·dC 2	13.14	12.87
dG·dC 4	12.75	12.73
dA·dT 5	13.97	13.79
dA·dT 6	13.86	13.79
	chemical shift (ppm)	
	dG·dC	dA·dC
position 3	12.96	

[a] Buffer: 0.1 M phosphate–H_2O, pH 7.5. [b] Buffer: 0.1 M phosphate–H_2O, pH 7.0.

the phosphorus NMR spectra.

Results

Imino Protons. The imino proton spectral region in the 12-mer AC duplex in 0.1 M phosphate–H_2O, −6 °C at pH 6.99 is shown in Figure 1A. The imino protons of the three dG·dC base pairs resonate at 13.24, 12.89, and 12.74 ppm while the imino protons of the two dA·dT base pairs are superimposed at 13.80 ppm. We do not observe any imino proton resonance from the dA·dC mismatch site between 9 and 14 ppm in the 12-mer AC duplex at this low temperature.

The imino proton at 13.24 ppm broadens out on raising the pH to 7.43 (Figure 1B) and is assigned to terminal dG·dC base pair 1 (Patel & Hilbers, 1975; Fritzsche et al., 1983). Inter base pair NOEs are observed between the imino protons of dA·dT base pairs 5 and 6 superimposed at 13.74 ppm and the dG·dC imino proton at 12.75 ppm (Figure 2B,D) but not the dG·dC imino proton at 12.91 ppm (Figure 2C) in the 12-mer

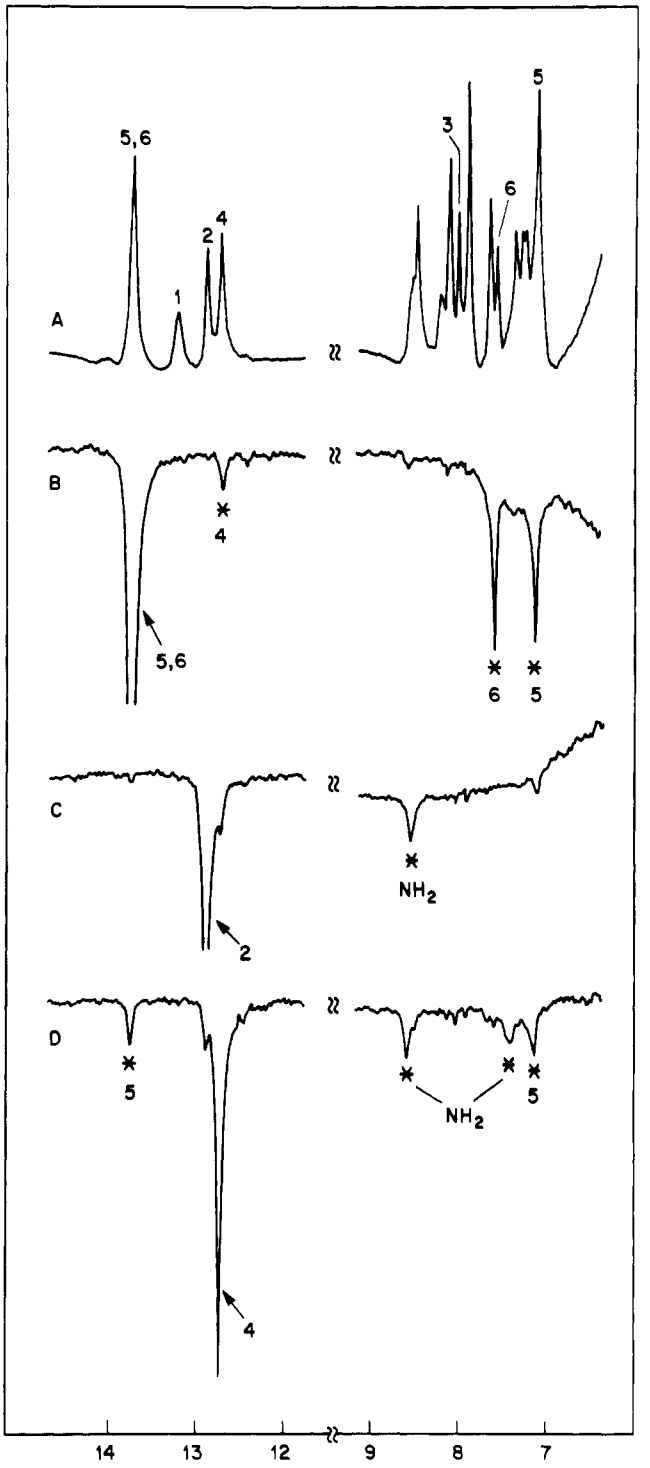

FIGURE 2: (A) The 498-MHz proton NMR spectra (12–14.5 ppm; 6.5–9 ppm) of the 12-mer AC duplex in 0.1 M phosphate, 2.5 mM EDTA, and 4:1 H_2O–D_2O, pH 6.99, at 5 °C. Difference spectra following 1-s saturation of (B) the 13.74 ppm thymidine imino protons of base pairs 5 and 6, (C) the 12.91 ppm guanosine imino proton of base pair 2, and (D) the 12.75 ppm guanosine imino proton of base pair 4. The saturated resonance is designated by an arrow while the observed NOEs are designated by asterisks.

AC spectrum at 5 °C. This permits the assignment of the 12.75 ppm imino resonance to base pair 4 and the 12.91 ppm imino resonance to base pair 2 in the 12-mer AC duplex at 5 °C. This completes the assignment of the imino resonances in the 12-mer AC duplex, and the chemical shifts at −6 °C are listed in Table I.

The temperature dependence of the imino proton spectra of the 12-mer AC duplex in 0.1 M phosphate, pH 6.99, is presented in Figure 3A between 0 and 40 °C. The imino

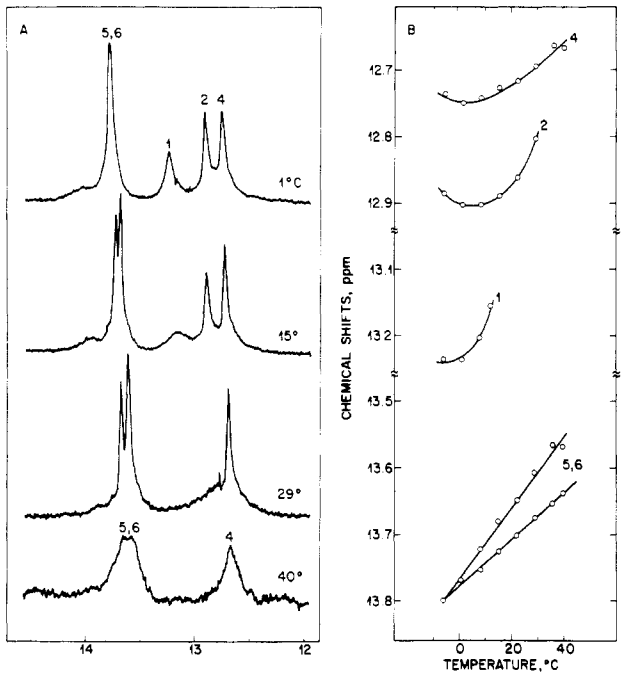

FIGURE 3: Temperature dependence of (A) the 498-MHz imino proton NMR spectra (12–14.5 ppm) and (B) the imino proton chemical shifts of the 12-mer AC duplex in 0.1 M phosphate, 2.5 mM EDTA, and 4:1 H_2O–D_2O, pH 6.99, between −6 and 40 °C.

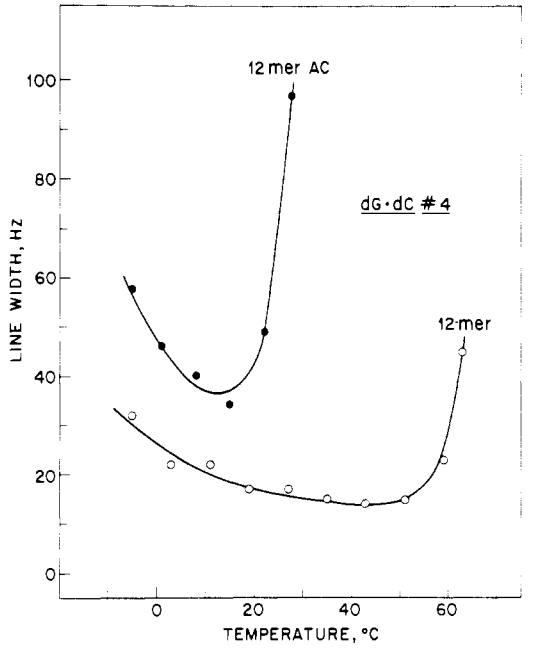

FIGURE 4: Temperature dependence of the line widths of the dG·dC base pair 4 imino protons for the 12-mer (○) and 12-mer AC (●) duplexes in 0.1 M phosphate and 4:1 H_2O–D_2O solution. The pH values were 7.50 (12-mer) and 7.43 (12-mer AC).

protons of base pairs 1 and 2 broaden by 15 and 30 °C, respectively, while the imino protons of base pairs 4–6 broaden simultaneously above 40 °C. The temperature dependence of the imino proton chemical shifts in the 12-mer AC duplex in this temperature range is plotted in Figure 3B. A comparison of the temperature dependence of the line width of dG·dC base pair 4 in the 12-mer and 12-mer AC duplexes (Figure 4) indicates that this imino proton exchanges much more rapidly with solvent H_2O when adjacent to a dA·dC mismatch site.

We have monitored the hydrogen-exchange kinetics of imino protons of base pairs 4–6 in the 12-mer AC duplex in 0.1 M phosphate, pH 6.90, as a function of temperature by the saturation-recovery method. A typical saturation-recovery run recorded at 26.2 °C yields first-order recoveries plotted for dA·dT base pairs 5 and 6 in Figure 5A and for dG·dC base pair 4 in Figure 5B. The saturation-recovery lifetimes at positions 4–6 in the 12-mer AC duplex in 0.1 M phosphate, pH 6.90, between 5 and 37.5 °C are listed in Table II and the corresponding Arrhenius plots of the data shown in Figure 6.

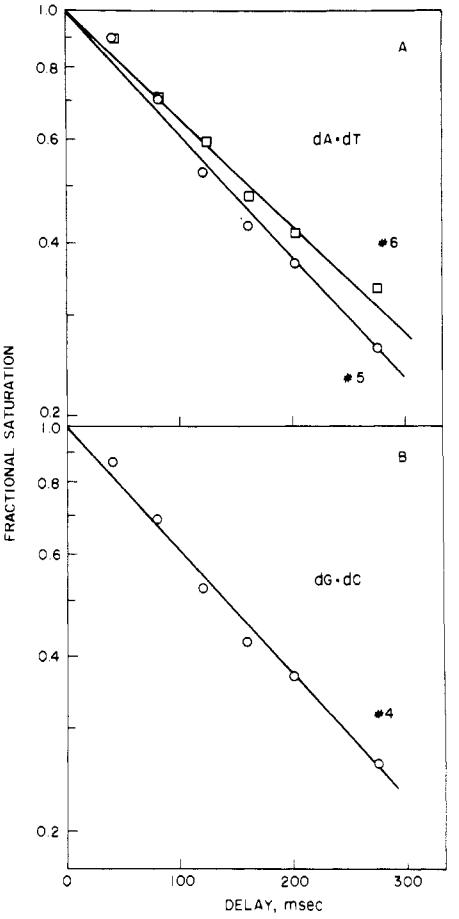

FIGURE 5: Recovery of magnetization plotted as the fractional saturation as a function of the delay between saturation and observation pulses for the imino protons of (A) dA·dT base pairs 5 and 6 and (B) dG·dC base pair 4 for the 12-mer AC duplex in 0.1 M phosphate, 2.5 mM EDTA, and 4:1 H_2O–D_2O, pH 6.90, at 26.2 °C.

Table II: Temperature and pH Dependence of the Saturation-Recovery Lifetimes of the Imino Protons in the 12-mer AC Duplex[a]

temp (°C)	imino proton lifetimes (ms) 4	5	6
	pH 6.90		
5.0	267	300	300
15.0	260	348	377
22.5	243	270	320
26.2	201	207	239
30.0	129	117	143
33.7	55	50	65
37.5	41	37	31
	pH 8.46		
26.2	34	45	59

[a] Buffer: 0.1 M phosphate, 2.5 mM EDTA, and 4:1 H_2O–D_2O.

Adenosine H-2 Protons. The resolution-enhanced nonexchangeable proton NMR spectrum of the 12-mer AC duplex in 0.1 M phosphate–D_2O at 15 °C between 5 and 9 ppm is presented in Figure 7. The three narrow adenosine H-2 protons in the 12-mer AC duplex can be readily identified since

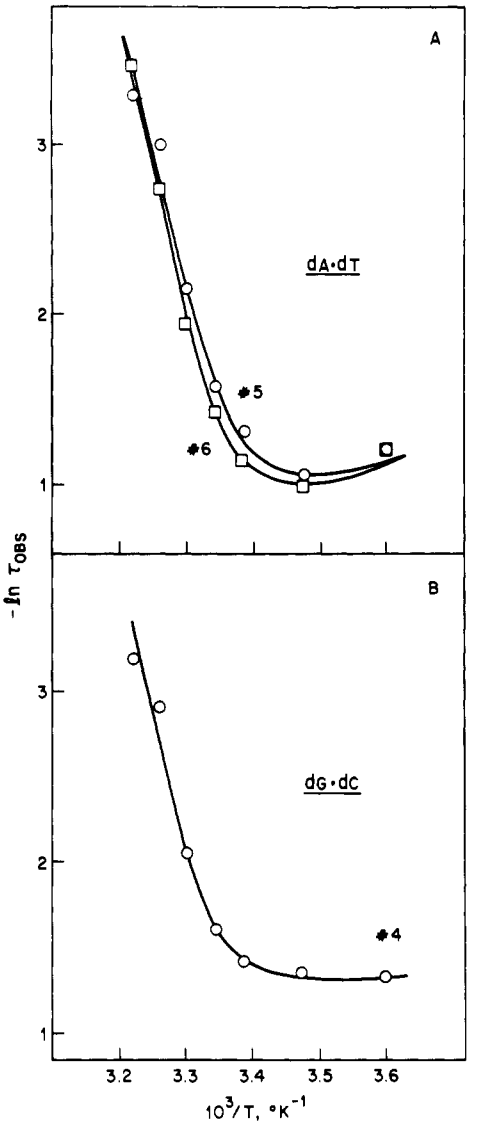

FIGURE 6: Arrhenius plots for the saturation-recovery rates for the imino protons of (A) dA·dT base pairs 5 and 6 and (B) dG·dC base pair 4 in the 12-mer AC duplex in 0.1 M phosphate, 2.5 mM EDTA, and 4:1 H_2O–D_2O, pH 6.90, between 5 and 37.5 °C.

they exhibit the longest spin–lattice relaxation times and resonate at 8.05, 7.60, and 7.16 ppm at 15 °C (Figure 7).

Saturation of the superimposed imino protons of dA·dT base pairs 5 and 6 at 13.74 ppm in the 12-mer AC spectrum in H_2O at 5 °C results in NOEs at the 7.57 and 7.12 ppm adenosine H-2 protons of base pairs 5 and 6 (Figure 2B). The remaining adenosine H-2 proton at 8.03 ppm must therefore be assigned to the adenosine at position 3 in the dA·dC mismatch site.

Saturation of the 12.75 ppm imino proton of dG·dC base pair 4 results in an inter base pair NOE at the 7.12 ppm adenosine H-2 of an adjacent dA·dT base pair (Figure 2D). This permits assignment of the 7.12 ppm adenosine H-2 to base pair 5 and the 7.57 ppm adenosine H-2 to base pair 6 in the 12-mer AC duplex at 5 °C.

The temperature dependence of the three adenosine H-2 protons in the 12-mer AC duplex in 0.1 M phosphate (closed circles) is compared with the two adenosine H-2 protons in the 12-mer duplex in 0.1 M phosphate (open circles) in Figure 8. The adenosine H-2 protons of dA·dT base pairs 5 and 6 show similar chemical shifts in the two duplexes and are upfield shifted from their strand values on duplex formation (Figure 8). By contrast, the adenosine H-2 in the dA·dC interaction exhibits a chemical shift of 8.05 ppm in the duplex state, which is similar to its value in the strand state (Figure 8).

Table III: One-Dimensional NOEs (ppm) among Base Protons of the 12-mer AC Duplex in 0.1 M Phosphate–D_2O at 5 °C

	NOEs observed at			
saturate	H-8	H-6	H-5	CH_3-5
		H-8		
8.52 (A3)		7.29 (C2)	5.42 (C2)	
8.15 (A5, A6)		7.15 (T6)		1.24 (T6)
7.93 (G1, G2, G4)		7.31 (C3)	5.66 (C3)	
		H-6		
7.67 (C1, C4)			5.86 (C1)	
			5.70 (C4)	
7.30 (C2, C3)	7.93		5.42 (C2)	
			5.66 (C3)	
7.40 (T5)			5.70 (C4)	1.52 (T5)
		CH_3-5		
1.52 (T5)		7.15 (T6)	5.70 (C4)	1.24 (T6)
		7.40 (T5)		
1.24 (T6)	8.15 (A6)	7.15 (T6)		1.52 (T5)

Table IV: Nonexchangeable Proton Chemical Shifts of the 12-mer and 12-mer AC Duplexes in 0.1 M Phosphate–D_2O Solution at 5 °C

		chemical shift (ppm)	
base pair	resonance	12-mer	12-mer AC
dA·dT 6	T(CH_3-5)	1.21	1.24
	T(H-6)	7.14	7.15
	A(H-2)	7.60	7.60
	A(H-8)	8.11	8.15
dA·dT 5	T(CH_3-5)	1.53	1.52
	T(H-6)	7.38	7.40
	A(H-2)	7.16	7.13
	A(H-8)	8.11	8.15
dG·dC 4	C(H-5)	5.62	5.70
	C(H-6)	7.46	7.67
	G(H-8)	7.86	7.93
dG·dC 2	C(H-5)	5.42	5.42
	C(H-6)	7.33	7.29
	G(H-8)	7.94	7.93
dG·dC 1	C(H-5)	5.91	5.86
	C(H-6)	7.61	7.67
	G(H-8)	7.94	7.93

Table V: Nonexchangeable Proton Chemical Shifts at Position 3 of the 12-mer and 12-mer AC Duplexes in 0.1 M Phosphate–D_2O Solution at 5 °C

	chemical shift (ppm)	
resonance	dG·dC	dA·dC
C(H-5)	5.35	5.66
C(H-6)	7.26	7.31
G(H-8)	7.91	
A(H-8)		8.52
A(H-2)		8.05

Base Proton Assignments. We have assigned the nonexchangeable base protons of dA·dT base pairs 5 and 6, dG·dC base pairs 1, 2, and 4, and dA·dC mismatch 3 from one-dimensional NOE experiments on the 12-mer AC duplex at 5 °C (Table III). The 12-mer AC base proton chemical shifts for the Watson–Crick base pairs are listed in Table IV while those for the dA·dC mismatch are listed in Table V.

The assignment procedure uses methods described previously and is based on NOEs between the purine H-8 and pyrimidine H-5 of adjacent bases on the same strand in the purine(3′–5′)pyrimidine step (inter proton distance <4 Å) but not in the pyrimidine(3′–5′)purine step (inter proton distance >4 Å). Thus, the thymidine base protons at position 5 can be dif-

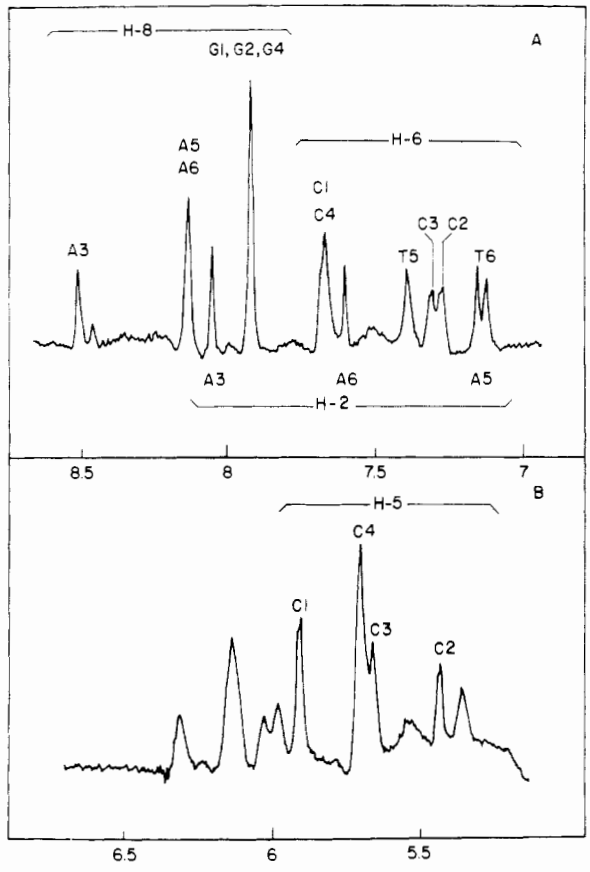

FIGURE 7: The 498-MHz proton NMR spectrum (5–8.5 ppm) of the 12-mer AC duplex in 0.1 M phosphate, 2.5 mM EDTA, and D_2O, pH 7.20, at 15 °C. The resolution of the spectrum was improved by a convolution difference of spectra with line broadening of 0 and 25 Hz. The pyrimidine H-5 and H-6 and adenosine H-2 protons have been completely assigned while the purine H-8 protons are partially assigned.

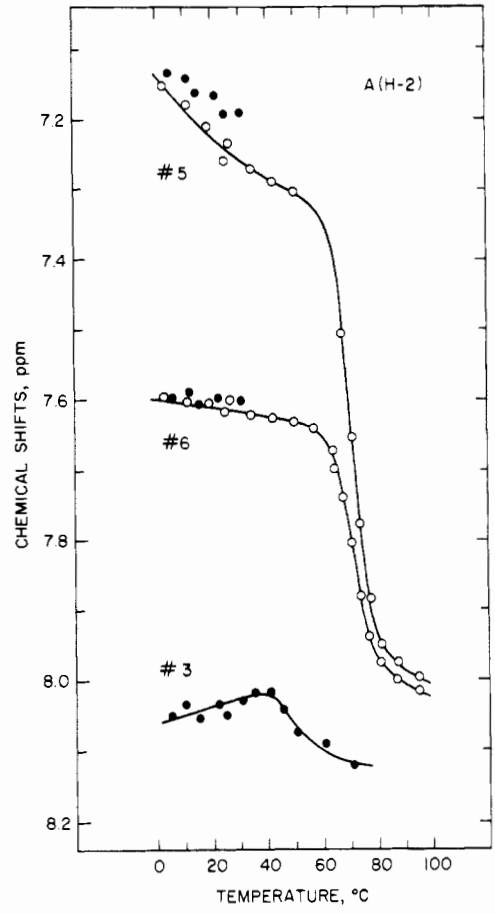

FIGURE 8: Temperature dependence of the chemical shifts of the adenosine H-2 protons at base pairs 5 and 6 in the 12-mer (○) and at base 3, 5, and 6 in the 12-mer AC (●) in 0.1 M phosphate–D_2O solution.

ferentiated from position 6 since the latter exhibits an NOE to the adenosine H-8 of position 6 in the A6(3′–5′)T6 step.

All four cytidines in 12-mer AC duplex have different bases in the 5′ direction [i.e., C1, G2(3′–5′)C3, T5(3′–5′)C4, and A3(3′–5′)C2] and, hence, can be differentiated on the basis of NOE measurements. We demonstrate this with an example involving the base protons in the A3(3′–5′)C2 step.

There are three adenosine H-8's in the 12-mer AC duplex with the two superpositioned resonances at 8.15 ppm (Figure 7) assigned to A5 and A6 since they exhibit the same chemical shift in the 12-mer, which has a common G4-A5-A6-T6-T5-C4 segment. This permits assignment of the downfield-shifted resonance at 8.52 ppm (Figure 7) to the adenosine H-8 of A3 at the mismatch site. Saturation for 1 s of the 8.52 ppm A3(H-8) resonance in the 12-mer AC duplex at 5 °C results in negative NOEs at the 5.42 ppm H-5 and 7.29 ppm H-6 resonances of an adjacent cytidine, which is assigned to residue 2 in an A3(3′–5′)C2 step (Figure 9B). This conclusion is confirmed by the observation of NOEs at the 8.52 ppm A3-(H-8) resonance and the 7.29 ppm C2(H-6) resonance on 1-s saturation of the 5.42 ppm C2(H-5) resonance in the 12-mer AC at 5 °C (Figure 9C). We have selectively saturated each of the base protons in turn and the observed NOEs are summarized in Table III, leading to the base proton assignments listed in Tables IV and V.

Melting Transition. We have monitored the duplex to strand transition of the 12-mer AC in 0.1 M phosphate by following the nonexchangeable base protons between 10 and 70 °C. The chemical shifts of the T6(H-6) resonance, the T5(CH_3-5) resonance, and the A3(H-8) resonance in the 12-mer (open circles) and the 12-mer AC (closed circles) are plotted in parts A, B, and C of Figure 10, respectively.

These resonances can be monitored as average peaks in the 12-mer duplex in 0.1 M phosphate and exhibit a transition midpoint of 72 °C (Patel et al., 1982b). By contrast, these resonances are in the intermediate to slow exchange in the 12-mer AC duplex in 0.1 M phosphate due to a drop in the transition midpoint to ~40 °C. Thus, the replacement of two dG·dC base pairs by two dA·dC base pairs results in an ~30 °C drop in the melting temperature of the dodecanucleotide duplex.

Phosphodiester Backbone. The phosphorus NMR spectra of the 12-mer AC duplexes in 33 mM phosphate buffer at 17 °C are presented in Figure 11. The most pronounced difference between the 12-mer (Patel et al., 1982b) and the 12-mer AC duplexes is the presence of a well-resolved phosphorus resonance at 3.76 ppm, downfield from the remaining phosphodiester dispersion between 4.0 and 4.5 ppm in the 12-mer AC duplex at 17 °C.

The temperature dependence of the phosphorus spectra of the 12-mer AC duplex in 33 mM phosphate between 17 and 50 °C is shown in Figure 11. The single phosphorus resonance at ~3.8 ppm and the cluster of resonances at ~4.45 ppm broaden in the 40 °C spectrum and coalesce into the remaining spectral region on raising the temperature to 50 °C (Figure 11).

Discussion

dA·dC Mismatch. The exchangeable proton NMR spectrum of the 12-mer AC duplex in 0.1 M phosphate, pH 6.99, at −6 °C exhibits five imino protons between 12 and 14 ppm

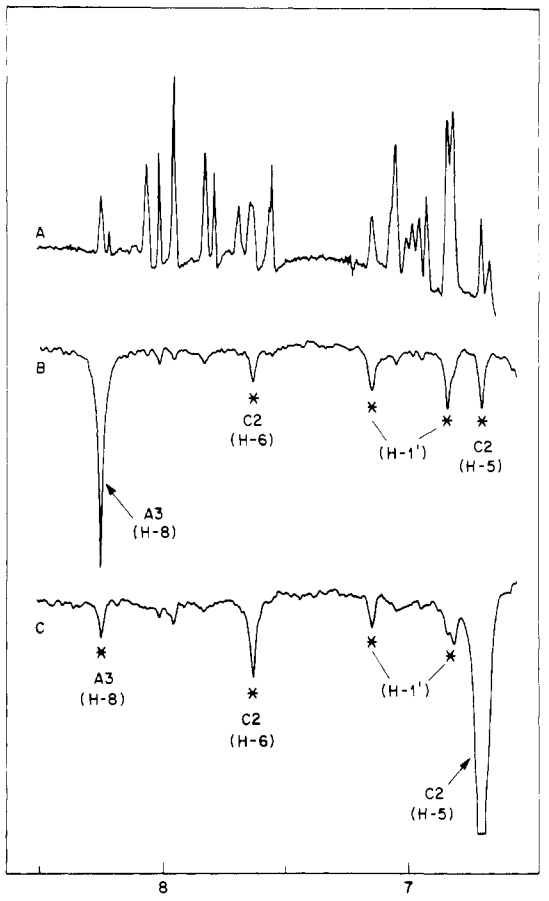

FIGURE 9: (A) The 498-MHz proton spectrum (6.5–8.5 ppm) of the 12-mer AC duplex in 0.1 M phosphate, 2.5 mM EDTA, and D_2O, pH 7.20, at 5 °C. The difference spectra following 1-s saturation of the 8.52 ppm adenosine H-8 resonance of base pair 3 and the 5.42 ppm cytidine H-5 of base pair 2 are shown in spectra B and C, respectively. The observed NOEs in the difference spectra are designated by asterisks. The signal to noise of spectra B and C was improved by applying a 10-Hz line-broadening contribution.

(Figure 1A), which have been assigned from NOE measurements (Figure 2) to the Watson–Crick dG·dC base pairs at positions 1, 2, and 4 and dA·dT base pairs at positions 5 and 6 (Table I). We do not observe a hydrogen-bonded imino proton in this region for the dA·dC mismatch since neither dA nor dC contains an imino proton in the keto form. We

Chart II

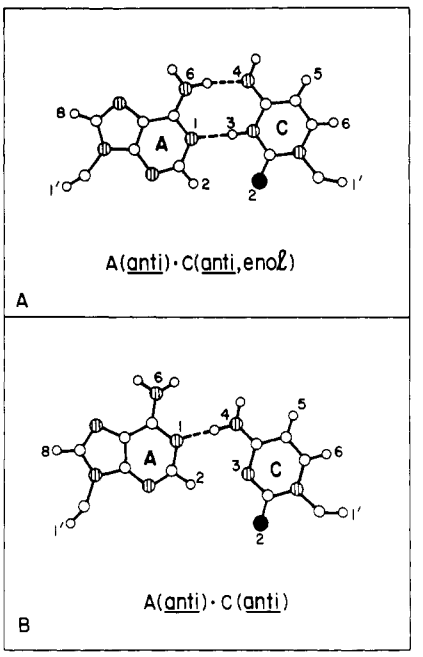

have also recorded the 12-mer AC spectrum in acetate buffer, pH 4.96, as a function of temperature and have not observed any hydrogen-bonded imino resonances between 14 and 12 ppm originating in the dA·dC mismatch at this acidic pH.

A possible dA·dC pairing scheme involving the enol tautomer of dC and both bases in anti configuration is presented in Chart IIA. The imino H-3 proton of dC(enol) is paired to the ring nitrogen 1 of dA, which should result in a hydrogen-bonded imino proton from the mismatch (Chart IIA) resonating in the 12–14 ppm region. Experimentally, we do not observe an imino proton from the mismatch site in the 12-mer AC duplex spectrum between pH 5 and 7 at low temperature, ruling against the pairing outlined in Chart IIA.

We do not experimentally observe inter base pair NOEs between the imino protons of dG·dC base pairs 2 and 4 and the adenosine H-2 at the dA·dC mismatch site 3 in the 12-mer AC duplex at low temperature (Figure 2C,D). This is in contrast to our experimental observations of such NOEs in the 12-mer GA duplex at low temperatures [see preceding paper (Patel et al., 1984)]. This suggests that the adenosine

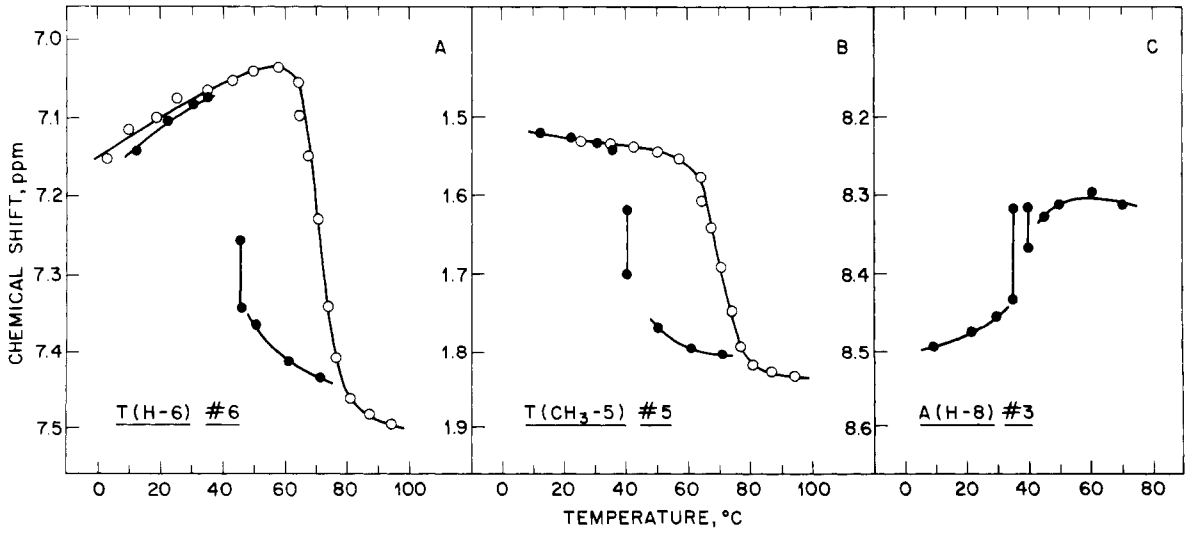

FIGURE 10: Temperature dependence of (A) base pair 6 thymidine H-6 chemical shift, (B) base pair 5 thymidine CH_3-5 chemical shift, and (C) base pair 3 adenosine H-8 chemical shift in the 12-mer (○) and the 12-mer AC (●) through the melting transition in 0.1 M phosphate solution.

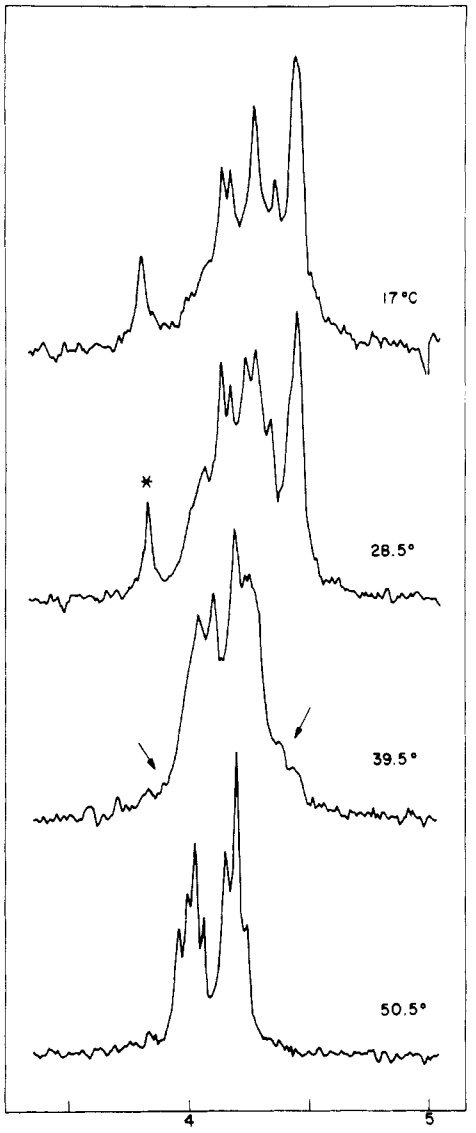

FIGURE 11: Proton noise decoupled 81-MHz phosphorus NMR spectra of the 12-mer AC in 33 mM phosphate, 0.8 mM EDTA, and D_2O, pH 7.22, between 17 and 50 °C. Chemical shifts are corrected for the temperature dependence of the internal standard trimethyl phosphate.

H-2 at position 3 in the dA·dC mismatch is >4 Å from the imino protons of adjacent base pairs 2 and 4 in the 12-mer AC duplex. One would have expected to observe these inter base pair NOEs for the dA·dC pairing outlined in Chart IIA since the orientation of the mismatch pair is similar to a Watson–Crick pair.

The adenosine base therefore has to slide out into the major or minor groove away from its position in the Watson–Crick pair. We can rule out partial sliding into the major groove since this would tend to orient the adenosine H-2 in the mismatch directly over the imino protons of adjacent dG·dC base pairs (Chart IIB). The predicted NOEs between these protons on adjacent base pairs for this orientation are not observed experimentally (Figure 2C,D). Further, the adenosine H-2 in the dA·dC mismatch at position 3 should exhibit a large upfield shift from ring-current contributions of adjacent base pairs for the orientation in Chart IIB in contrast to experimental results where the adenosine H-2 undergoes a negligible upfield shift on 12-mer AC duplex formation (Figure 8).

By contrast, partial sliding of the adenosine base of the dA·dC mismatch into the minor groove would result in a

Chart III

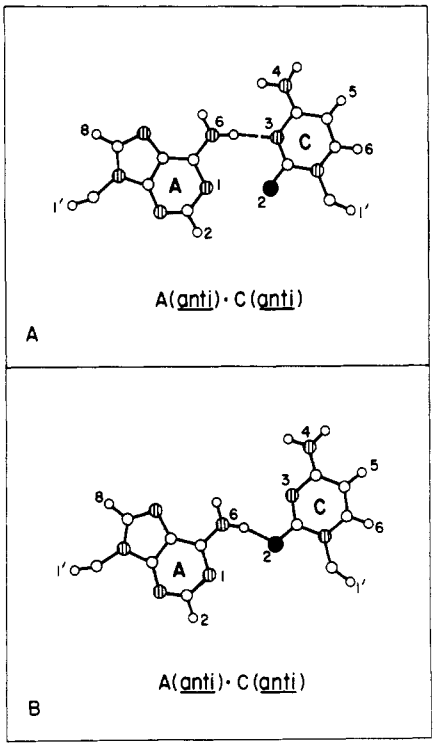

significant increase in the distance of its adenosine H-2 proton from the imino protons of adjacent dG·dC base pairs. Such a sliding is schematically represented in Chart III and would account for the absence of inter base pair NOEs between the adenosine H-2 at the dA·dC mismatch and the imino protons of adjacent dG·dC base pairs 2 and 4 (Figure 2C,D).

The proposed dA·dC pairing is stabilized by a single intramolecular hydrogen bond between the amino H-6 proton of adenosine and either the ring nitrogen 3 of cytidine (Chart IIIA) or the carbonyl oxygen 2 of cytidine (Chart IIIB). The pairing can be visualized as the adenosine base sliding out partly into the minor groove and the cytidine base sliding out partly into the major groove, similar to what happens on wobble dG·dT base-pair formation. The extent of sliding to form the dA·dC mismatch differs in parts A and B of Chart III with a larger change for the latter orientation. We are unable to differentiate between these two possibilities at this time.

We also note that the adenosine H-2 proton at the dA·dC mismatch site resonates at 8.05 ppm in contrast to chemical shifts of 7.6 and ~7.2 ppm for dA·dT base pairs 6 and 5 in the 12-mer AC duplex (Figure 8). The absence of an upfield shift for the adenosine H-2 in the dA·dC mismatch suggests that this proton does not stack over the aromatic rings of adjacent base pairs in the 12-mer AC duplex. This condition is met by the adenosine H-2 of the mismatch pairing represented in Chart III since the adenosine base has partly swung out into the minor groove.

We cannot rule out the possibility that one or both bases at the mismatch site are not stacked but are looped out in solution. The looping out of the adenosine base is consistent with the downfield shifts of the purine H-2 and H-8 protons at the mismatch site (Table V) and the absence of inter base pair NOEs noted in the difference spectra in Figure 2.

The dG·dC base pairs 2 and 4 could stack on each other if both bases at the mismatch site 3 loop out into solution. The predicted inter base pair NOE between the imino protons of base pairs 2 and 4 for this configuration cannot be checked

by one-dimensional NOE experiments since these imino protons are separated by 0.15 ppm and saturation of one results in spillover to the other (Figure 2). This ambiguity may be resolved by future two-dimensional NOE measurements on the 12-mer AC duplex.

Exchange Behavior. We observe a sequential broadening of the imino protons of dG·dC base pairs 1 and 2 of the 12-mer AC duplex in 0.1 M phosphate, pH 7, on raising the temperature to 15 and 30 °C, respectively (Figure 3A). The line widths of these imino protons in the 12-mer AC duplex also broaden on raising the pH (Figure 1). These observations are consistent with fraying at the ends of the 12-mer AC duplex below room temperature (Patel & Hilbers, 1975; Fritzsche et al., 1983). The imino protons of base pairs 4–6 broaden simultaneously above 40 °C (Figure 3A) with the onset of the melting transition.

We have compared the line width of the imino proton of dG·dC base pair 4 in the 12-mer and 12-mer AC duplexes in 0.1 M phosphate at pH ~7.5. The imino proton at this position broadens out at ~65 °C in the 12-mer but does so at ~25 °C in the 12-mer AC duplex. This difference is larger than the ~30 °C difference in the transition midpoints between the 12-mer and 12-mer AC duplexes. This is indicative of a kinetic destabilization adjacent to the mismatch site on replacing a dG·dC base pair by a dA·dC base pair.

We have quantitated the hydrogen-exchange behavior of the imino protons of base pairs 4–6 from saturation-recovery measurements on the 12-mer AC duplex in 0.1 M phosphate, pH 6.99, between 5 and 37.5 °C (Table II). The Arrhenius plots of the saturation-recovery lifetimes (Figure 6) are predominately a measure of hydrogen exchange above 22.5 °C and a measure of spin–lattice relaxation below this temperature (Early et al., 1981a,b; Pardi & Tinoco, 1982; Pardi et al., 1982).

We have compared the pH dependence of the saturation-recovery lifetimes of the imino protons at positions 4–6 in the 12-mer AC in 0.1 M phosphate at pH 6.9 and 8.46 at 26.2 °C (Table II). The saturation-recovery lifetimes exhibit a pronounced dependence on pH with the lifetimes decreasing by a factor of ~6 at base pair 4 and a factor of ~4 at base pairs 5 and 6 on raising the base concentration by a factor of ~15. The dependence of the hydrogen exchange on base concentration suggests that both the helix-opening and preequilibrium pathways contribute to hydrogen exchange at base pairs 4–6 in the 12-mer AC duplex.

We have compared the saturation-recovery lifetime of the imino protons of dA·dT base pairs 4–6 in the 12-mer and 12-mer AC duplexes in 0.1 M phosphate, neutral pH, at 30 °C (Table VI). The replacement of dG·dC base pairs at position 3 by dA·dC pairs results in a kinetic destabilization of a factor of ~3 at adjacent dG·dC base pair 4 and a factor of ~2 at dA·dT base pairs 5 and 6. This contrasts with our hydrogen-exchange results in the 12-mer GT (Pardi et al., 1982) and 12-mer GA [see preceding paper (Patel et al., 1984)] duplexes where the kinetic destabilization was localized at base pair 4 and did not extend to base pairs 5 and 6 in the interior of the duplex.

The activation barriers estimated directly from the slope of the saturation-recovery data between 26.2 and 37.5 °C give activation energies at positions 4–6 in the 12-mer AC duplex, which are a factor of 2 larger than the corresponding values in the 12-mer duplex (Table VI). This suggests that hydrogen exchange at these positions proceeds through the cooperative opening of several base pairs in the 12-mer AC duplex similar to what was observed earlier for the 12-mer GT (Pardi et al., 1982) and 12-mer GA [see preceding paper (Patel et al., 1984)] duplexes.

Table VI: A Comparison of the Imino Proton Lifetimes (30 °C) and the Saturation-Recovery Activation Barriers for the 12-mer (pH 6.95) and the 12-mer AC (pH 6.99) Duplexes in 0.1 M phosphate, 2.5 mM EDTA, and 4:1 H_2O–D_2O Solution

	imino proton lifetimes (ms) at 30 °C		
	4	5	6
12-mer	358	184	310
12-mer AC	129	117	143
	saturation-recovery barriers (kcal)[a]		
	4	5	6
12-mer		17	17.5
12-mer AC	31	32	35

[a] The activation barriers were directly computed from the slope of the saturation-recovery data between 30 and 40 °C (Figure 7).

Base Stacking. The imino protons of dG·dC pairs 2 and 4 on either side of the mismatch site can be readily detected in the 12-mer AC spectrum at low temperature (Figure 1A), consistent with intact Watson–Crick base-pair formation. It was therefore of interest to compare the base proton chemical shifts adjacent to (base pairs 2 and 4) and far from (base pairs 1, 5, and 6) the mismatch site in the 12-mer AC with those of the 12-mer duplex (Table IV).

We observe several differences in the chemical shifts of the 12-mer and 12-mer AC base protons listed in Tables I and IV. The imino protons of dG·dC base pair 2 adjacent to the dA·dC mismatch site and dA·dT base pair 5 one removed from the mismatch shift to high field on proceeding from the 12-mer to the 12-mer AC duplex at −5 °C (Table I).

The cytidine H-6 proton and, to a lesser extent, the cytidine H-5 proton of dG·dC base pair 4 are the only nonexchangeable protons that are perturbed and shift downfield on proceeding from the 12-mer to the 12-mer AC duplex (Table IV). This may reflect less overlap of these pyrimidine base protons with the adjacent adenosine in the mismatch, which replaces the guanosine in the standard pair.

The orientation of the cytidine base at position 3 with respect to adjacent base pairs is different in the dA·dC mismatch compared to the dG·dC pair since the cytidine H-5 proton shifts 0.3 ppm downfield on going from the 12-mer to the 12-mer AC duplex (Table V). The adenosine H-8 proton (8.52 ppm) in the dA·dC mismatch (Table V) is downfield from the corresponding values (8.11 ppm) for dA·dT base pairs 5 and 6 (Table IV). Thus, the cytidine H-5, adenosine H-8, and adenosine H-2 protons at the dA·dC mismatches are all shifted to low field compared to typical values for standard base pairs. This may reflect the fact that there is less overlap between adjacent base pairs and the mismatch bases.

Protonation of the adenosine ring could also account for the observed downfield chemical shift of the adenosine H-8 and H-2 protons at the dA·dC mismatch site. We note that the proposed dA·dC pairing outlined in Chart IIIA would permit a hydrogen bond between a protonated adenosine N-1 proton and the cytidine O-2 carbonyl group. The exchange of this protonated hydrogen-bonded N-1 proton located at the edge of the dA·dC base pair could be too fast to be observable as a narrow resonance in the NMR spectrum between 10 and 15 ppm, even at low temperature.

Phosphodiester Backbone. The observed differences between the phosphorus spectra of the 12-mer (Patel et al., 1982b) and the 12-mer AC (Figure 11) duplexes cannot be

quantitated due to lack of assignments to specific positions in the sequence. The downfield-shifted 3.76 ppm resonance in the 12-mer AC spectrum at 17 °C (Figure 11), which has no counterpart in the 12-mer spectrum at the same temperature, is tentatively assigned to a phosphodiester at the mismatch site. This suggests a difference in the conformation (Gorenstein, 1981; Patel et al., 1982a) of at least one phosphodiester residue between the 12-mer and 12-mer AC duplexes.

Overall Stability. The relative stability of different base-pair mismatches can be evaluated from a comparison of the helix–coil transition midpoints of the 12-mer duplex in 0.1 M phosphate (72 °C) (Patel et al., 1982b) with the corresponding values for the 12-mer GT (~52 °C) (Patel et al., 1982a), 12-mer GA (~55 °C) [preceding paper (Patel et al., 1984)], and 12-mer AC (~40 °C) in the same buffer. It is apparent that replacing two dG·dC base pairs in the dodecanucleotide by either two dG·dT or two dG·dA pairs results in a comparable destabilization of 17–20 °C while replacement by two dA·dC pairs results in a larger destabilization of ~ 30 °C. This suggests that dG·dT and dG·dA mismatches can be more readily accommodated into DNA duplexes than can a dA·dC mismatch.

Molecular Mechanics Calculations. J. W. Keepers, P. Schmidt, and P. A. Kollman (unpublished results) report on their molecular mechanics calculations on the 12-mer AC duplex. These workers observe a low-energy conformation for the 12-mer AC duplex that involves hydrogen-bonding between the adenosine NH_2 group at position 6 and the cytidine ring nitrogen at position 3 at the dA·dC mismatch site without disruption of adjacent base pairs. The conclusions concerning dA·dC pairing presented in our NMR paper support the computational conclusions of J. W. Keepers, P. Schmidt, and P. A. Kollman (unpublished results) that dA·dC pairing may involve hydrogen-bonding interactions as outlined in Chart IIIA (or Chart IIIB) but disagree with the computational conclusions of Rein et al. (1983), who favor hydrogen-bonding interactions outlined in Chart IIB. Two-dimensional NMR studies are in order to either support or rule out the possibility that both bases at the dA·dC mismatch site may be looped out into solution.

Acknowledgments

We acknowledge helpful discussions with Dr. Horace Drew on potential pairing modes for the dA·dC mismatch pair.

References

Early, T. A., Olmsted, J., III., Kearns, D. R., & Lezius, A. G. (1978) *Nucleic Acids Res. 5*, 1955–1970.

Early, T. A., Kearns, D. R., Hillen W., & Wells, R. D. (1981a) *Biochemistry 20*, 3756–3764.

Early, T. A., Kearns, D. R., Hillen, W., & Wells, R. D. (1981b) *Biochemistry 20*, 3764–3769.

Fritzsche, H., Kan, L. S., & Tso, P. O. P. (1983) *Biochemistry 22*, 277–280.

Gorenstein, D. G. (1981) *Annu. Rev. Biophys. Bioeng. 10*, 355–386.

Kan, L., Chandrasekaran, S., Pulford, S. M., & Miller, P. S. (1983) *Proc. Natl. Acad. Sci. U.S.A. 80*, 4263–4265.

Lomant, A. J., & Fresco, J. R. (1975) *Prog. Nucleic Acid Res. Mol. Biol. 15*, 185.

Pardi, A., & Tinoco, I., Jr. (1982) *Biochemistry 21*, 4686–4693.

Pardi, A., Morden, K. M., Patel, D. J., & Tinoco, I., Jr. (1982) *Biochemistry 21*, 6567–6574.

Patel, D. J., & Hilbers, C. W. (1975) *Biochemistry 14*, 2651–2656.

Patel, D. J., Kozlowski, S. A., Marky, L. A., Rice, J. A., Broka, C., Dallas, J., Itakura, K., & Breslauer, K. (1982a) *Biochemistry 21*, 437–444.

Patel, D. J., Kozlowski, S. A., Marky, L. A., Broka, C., Rice, J. A., Itakura, K., & Breslauer, K. J. (1982b) *Biochemistry 21*, 428–436.

Patel, D. J., Kozlowski, S. A., Ikuta, S., & Itakura, K. (1984) *Biochemistry* (preceding paper in this issue).

Redfield, A. G., Roy, S., Sanchez, V., Tropp, J., & Figueroa, N. (1981) in *Second SUNYA Conference on Biomolecular Stereodynamics* (Sarma, R. H., Ed.) pp 195–208, Adenine Press, New York.

Reid, B. R. (1981) *Annu. Rev. Biochem. 50*, 969.

Rein, R., Shibata, M., Garduno-Juarez, R., & Kieber-Emmons, T. (1983) in *Structure and Dynamics: Nucleic Acids and Proteins* (Clementi, E., & Sarma, R. H., Eds.) pp 269–288, Adenine Press, New York.

Tan, Z. K., Ikuta, S., Huang, T., Dugaiczyk, A., & Itakura, K. (1983) *Cold Spring Harbor Symp. Quant. Biol. 47*, 383–391.

Wallace, R. B., Shaffer, J., Murphy, R. F., Bonner, J., Hirose, T., & Itakura, K. (1979) *Nucleic Acids Res. 6*, 3543–3557.